

A Quantitative Comparison of Metabolite Signals as Detected by *in-vivo* MRS with *ex-vivo* ^1H HR-MAS for Childhood Brain Tumours.

Martin Wilson^{1,2}, Nigel P Davies^{3,1,2}, Richard G Grundy⁴, Andrew C Peet^{1,2}

¹ Academic Department of Paediatrics and Child Health, University of Birmingham, UK.

² Birmingham Children's Hospital NHS Foundation Trust, Birmingham, UK.

³ Medical Physics and Imaging, University Hospital Birmingham, Birmingham, UK.

⁴ The Childhood Brain Tumour Research Centre, The Medical School, Nottingham University, Nottingham, UK.

Correspondence to: Martin Wilson, Academic Department of Paediatrics and Child Health, Birmingham Children's Hospital, Steelhouse Lane, Birmingham, West Midlands, B4 6NH, UK, Tel No.: 01213338744, Email to: martin@pipegrep.co.uk.

Running title: A quantitative comparison of *in-vivo* MRS with *ex-vivo* ^1H HR-MAS.

Key words: HR-MAS, ^1H , MRS, brain, tumour, pediatric, TARQUIN, LCMModel.

Abbreviations

Ala	Alanine
Asp	Aspartate
Cho	Choline
Cr	Creatine
CRLB	Cramer-rao lower bound
FWHM	Full width at half maximum
Gln	Glutamine
Glu	Glutamate
Glx	Glutamate and glutamine
Gly	Glycine
GPC	Glycero-phosphocholine
H&E	Hematoxylin and eosin
^1H HR-MAS	^1H High resolution magic angle spinning
Ins	Myo-inositol
Lac	Lactate
MB	Medulloblastoma
NAA	N-Acetylaspartate
PEth	Phosphorylethanolamine
Pilo. astrocytoma	Pilocytic astrocytoma
PC	Phosphocholine
Scyllo	Scyllo-inositol
SNR	Signal-to-noise ratio
SVS	Single voxel spectroscopy
Tau	Taurine
TCho	Total choline
TSP	3-(trimethylsilyl)propionic-2,2,3,3-d ₄ acid sodium salt
WHO	World health organisation

Abstract

^1H MRS provides a powerful method for investigating tumour metabolism by allowing the measurement of metabolites *in-vivo*. More recently the technique of ^1H High-Resolution Magic Angle Spinning (HR-MAS) has been shown to produce high quality data allowing the accurate measurement of many metabolites present in unprocessed biopsy tissue. The purpose of this study was to evaluate the agreement between the techniques of *in-vivo* MRS and *ex-vivo* HR-MAS for investigating childhood brain tumours. Short echo time (30ms), single voxel, *in-vivo* MRS was performed on 16 paediatric brain tumour patients at 1.5T. A frozen biopsy sample was available for each patient. HR-MAS was performed on the biopsy samples and metabolite quantities were determined from the MRS and HR-MAS data using the LCMoDelTM and TARQUIN algorithms respectively. Linear regression was performed on the metabolite quantities to assess the agreement between MRS and HR-MAS. 8 of the 12 metabolite quantities were found to be significantly correlated ($p < 0.05$). The four worst correlating metabolites were aspartate, scyllo-inositol, glycerophosphocholine and n-acetylaspartate and, with the exception of glycerophosphocholine, this error was reflected in their higher Cramer-Rao lower bounds (CRLBs) suggesting that low signal to noise was the greatest source of error for these metabolites. Glycerophosphocholine had a lower CRLB implying that interference with phosphocholine and choline was the most significant source of error. The generally good agreement observed between the two techniques suggests that both MRS and HR-MAS can be used to reliably estimate metabolite quantities in brain tumour tissue and that tumour heterogeneity and metabolite degradation do not have an important effect on the HR-MAS metabolite profile for the tumours investigated. HR-MAS can be used to improve the analysis and understanding of MRS data.

1 Introduction

In-vivo ^1H Magnetic Resonance Spectroscopy (^1H MRS) is a powerful non-invasive method for measuring the concentration of biochemicals in a pre-selected volume of interest. The biochemical profiles measured by ^1H MRS have been used to diagnose and characterise a variety of diseases (1, 2, 3, 4, 5, 6, 7). Non-invasive methods are of particular clinical importance in the study of childhood brain tumours and ^1H MRS has been shown to provide information on tumour type, grade and prognosis (8, 9, 7) as well as being a promising tool for treatment monitoring. Short echo time ^1H MRS is particularly useful in characterising childhood brain tumours (8, 7), most likely due to the increased number of metabolites which can be detected compared with long echo time MRS. However, at the field strengths typically used for clinical *in-vivo* ^1H MRS (around 1.5 Tesla), many metabolite and macromolecular signals strongly overlap in short echo time ^1H MRS making the accurate quantitation of many biochemicals difficult. LCModelTM (10) has become a well accepted method for the automated quantitation of metabolites from *in-vivo* ^1H MRS and gives values for approximately 15 metabolites from short echo time ^1H MRS. However, little information is available on the accuracy of this metabolite assignment and quantitation for brain tumours due to the difficulty in determining the true metabolite concentrations *in-vivo*.

The problem of overlapping signals is less pronounced for tumour tissue analysed *ex-vivo* using ^1H High-Resolution Magic Angle Spinning (HR-MAS) and this technique has the potential to aid assignment and quantitation of *in-vivo* ^1H MRS. A combination of higher field strength (typically 14.1T) and mechanically spinning the sample about the magic angle gives an order of magnitude improvement in spectral resolution when compared to *in-vivo* ^1H MRS. These properties have led to HR-MAS emerging as an important technique in the field of cancer research in its own right. Recent studies have used ^1H HR-MAS to investigate a variety of tissues including diseased brain (11), breast tumour (12, 13), cervical carcinoma (14), liver

tumour (15, 16), primary (17, 18, 19) and metastatic (20) adult brain tumours and paediatric brain tumours (21, 22).

Good quality HR-MAS data can be obtained from small pieces of tissue (5mg) which is a significant advantage for childhood brain tumour research where tissue samples available from operation are commonly small. However, the use of small sample sizes introduces the risk of the sample not being representative of the whole tumour. Ideally, experiments should be performed on multiple samples taken from the tumour mass. However, for childhood brain tumours there are commonly competing demands on tissue in terms of diagnosis and other molecular investigations. When interpreting HR-MAS on excised tissue it is also important to consider the extent to which removing the tissue from the body alters the HR-MAS profile. While assessment of adult brain tumour and rat brain have shown metabolite degradation to be minimal (17, 23), these effects may be tissue and time (between removal and snap freezing) dependent.

Whilst *in-vivo* ^1H MRS and HR-MAS are powerful tools for the investigation of childhood brain tumours, both have potential sources of inaccuracy and the assessment of these is important to the further development of these methods. Consistent data quality and accurate automated signal analysis still represent significant challenges to *in-vivo* ^1H MRS achieving its full potential as a clinical tool. The issues of tumour heterogeneity and metabolite degradation are important for interpretation of HR-MAS. The purpose of this study is to evaluate the agreement between the metabolite quantities measured by *in-vivo* ^1H MRS and *ex-vivo* HR-MAS from a cohort of paediatric brain tumour cases. Whilst this is not a formal validation of either technique, areas of agreement will give some measure of the reliability of the techniques while areas of disagreement will give insight into practical limitations. Similar comparisons have been published, but results have only been presented on three metabolite quantities (21), or have only been qualitative (19). The emergence of accurate methods for the quantitation of multiple metabolites from HR-MAS data

(24) allows a quantitative comparison over the full range of metabolites.

2 Method

2.1 Cohort Details

The cohort was taken from eligible patients undergoing MR imaging at Birmingham Children’s Hospital as part of their clinical investigations for a suspected brain tumour. For a patient to be eligible for entry into the study, it was required that pre-treatment *in-vivo* short echo SVS be available and that corresponding pre-treatment ^1H HR-MAS had been performed on the same tumour. All patients underwent a major surgical resection as part of the clinical management of their tumour. Approval for the study was obtained from the research ethics committee and informed consent taken from parents/guardians. Samples obtained at surgery from all patients were subjected to histopathological examination to obtain a diagnosis according to the WHO classification (25). This diagnosis was reviewed and agreed by the clinical multi-disciplinary team at Birmingham Children’s Hospital.

2.2 *In-vivo* MRS

MRI and MRS were carried out on a 1.5T Siemens Symphony Magnetom. Standard imaging included T1 and T2 weighted images of the brain followed by gadolinium contrast administration and then T1 weighted images of the head and spine where appropriate. The conventional imaging set was used to delineate the margins of the primary tumour and the voxel for MRS was placed entirely within this region encompassing as much of the solid component of the tumour as possible. Point resolved single voxel spectroscopy was performed with an echo time of 30 ms and a repetition time of 1500ms. Cubic voxels of either 2cm or 1.5cm length were used depending on the size of the tumour. Water suppressed data was acquired with 128 repetitions from the larger voxels and 256 repetitions from the smaller ones. Water

unsuppressed data was also acquired for eddy current correction. The raw MRS signals were processed using the LCModelTM software package (version 6.0-1) (10).

2.3 *Ex-vivo* HR-MAS

Biopsy tissue, selected by a histopathologist from tumour collected as part of a major surgical resection, was snap frozen in liquid nitrogen shortly after resection and stored at -80°C. Just prior to ¹H HR-MAS, tissue was thawed at room temperature and cut to approx 15mg where available. The tissue was then placed into a 40μL wide mouth zirconia rotor and weighed. 4μL of TSP was dissolved in D₂O at a concentration of 10mM and was added to the rotor. The remaining volume of the rotor was filled with D₂O to ensure constant spinning for each sample. ¹H HR-MAS was performed on a Varian 600MHz vertical bore spectrometer using a 4mm gHX nanoprobe (Varian NMR Inc, Palo Alto, CA, USA) with a 3 channel Inova console running VNMRj software. The probe temperature was set to 0.1°C to minimise sample degradation, and the sample was spun at 2500Hz. These conditions yielded a sample temperature of 6.7°C determined by methanol calibration.

A standard pulse and acquire sequence was used which consisted of a single 90° pulse preceded by one second of water presaturation. The 90° pulse was followed by the acquisition of 16K complex points at a sampling frequency of 7200Hz. 512 scans were acquired with a repetition time of 3.3 seconds giving a total acquisition time of 28 mins. A 30-ms CPMG pulse sequence was also used to aid metabolite assignment. This consisted of an xy 16 hard pulse train with a 1-s water presaturation pulse; the rotor speed was 2500Hz; 512 scans gave a 28-min acquisition time. Tuning and matching, 90° pulse width and the presaturation pulse frequency were optimised for each sample.

Raw data was Fourier transformed to 16K points, phased and referenced to the creatine peak at 3.03ppm using in house software¹. The phased data was then

¹available from <http://sourceforge.net/projects/dangerplotpy>

transformed back to the time-domain and a modified version of the TARQUIN algorithm (24) was used to fit the metabolite components of the signal.

2.4 Statistical Analysis

Statistical analysis was performed on data which passed QC criteria. Initially, all *in-vivo* data was fitted using LCModel and spectra with a signal-to-noise ratio, $\text{SNR} < 6$ and full width at half maximum, $\text{FWHM} > 0.14$ were deemed to be of poor quality and eliminated from further analysis. The values for SNR and FWHM were calculated by LCModel as part of the fitting process. The average CRLBs were calculated by LCModel for each fitted metabolite and were used as an estimate of the random error of the metabolite quantities. Note that for cases where the metabolite quantity is zero the CRLB is meaningless and so these values were not included in the average.

Myo-inositol, creatine and total choline all have CRLBs of less than 20% and so metabolite quantities were divided by the sum of these three signals. In addition to these, glycine was also included in the summation for the ^1H HR-MAS data as this signal was not present in the LCModel basis set, and is known to overlap with myo-inositol at 1.5T.

As water reference data was unavailable for ^1H HR-MAS data, the *in-vivo* MRS and *ex-vivo* ^1H HR-MAS metabolite quantities were scaled as follows to allow a direct comparison. *in-vivo* metabolite amplitudes as determined by LCModel were scaled by the sum of Ins, Cr and TCho since the quantitation of those metabolites was most robust as reflected by their small average CRLB ($< 20\%$). To ensure consistency, the same scaling method was used for ^1H HR-MAS data with the exception that Gly was also included as it cannot be separated from Ins *in-vivo* with short TE MRS, whereas it is can be resolved in the high resolution *ex-vivo* spectra. This procedure was undertaken to ensure that the random variation of poorly fitted metabolites *in-vivo* did not interfere with scaling. Finally, linear regression was performed for

each metabolite using the Gnumeric software package (26).

3 Results and Discussion

16 patients met the study entry requirements specified in section 2.1. Of these, 15 patients (8 medulloblastoma, 5 pilocytic astrocytoma and 2 ependymoma) passed the *in-vivo* MRS quality control requirements. The average FWHM was found to be 0.07ppm and the average SNR was 17.9, as determined by the LCModel analysis (10). Figure 1 gives the average CRLB for each metabolites which shows that creatine, myo-inositol and total choline have the lowest estimated error and consequently were used to scale the other metabolite quantities.

Table 1 shows that of the 12 metabolites tested, 8 were significantly correlated with a p-value of less than 0.05. A spectral comparison also showed good agreement, and an example is plotted in figure 2. This result demonstrates that short echo SVS can be used to reliably measure quantities of a number biochemicals present in brain tumour tissue. One of the major issues surrounding short echo data at 1.5T is that the overlap of signals can hamper quantitation. The results presented imply that despite being heavily overlapped, LCModel can differentiate between glutamate and glutamine for the tumours investigated. This result is perhaps surprising given the relatively minor differences between these signals at 1.5T, however this result may be explained by a large variation of these two metabolites across the tumours studied resulting in greater distinction. The general agreement between the methods also demonstrates that tumour inhomogeneity and metabolite degradation are not a major determinant of the ^1H HR-MAS metabolite profile for the tumours investigated. This finding is not likely to be replicated in tumours with high levels of intratumoural heterogeneity such as glioblastoma multiforme in adults and emphasises the importance of tumour specific investigations. The results give support to the strategy of translating hypotheses generated by ^1H HR-MAS to *in-vivo* using

short echo time SVS.

The intercept of the linear regression line for lactate has a significant deviation from zero, a result which can be explained since it is known that lactate is elevated *ex-vivo* due to the degradation of glucose and glycogen (23). Despite having an intercept of -0.23, lactate levels detected *in-vivo* and *ex-vivo* correlate with a very high significance ($p=0.0002$). This shows that while lactate levels are elevated *ex-vivo* they are proportional to those seen *in-vivo* and can still be used to gain insight into the metabolism *in-vivo*.

The intercept of the linear regression line for myo-inositol also shows a large deviation (0.3) from zero which is shown in figure 4. This deviation can be reduced by adding glycine to myo-inositol in the ^1H HR-MAS data, as shown in figure 5. Adding glycine also leads to a significant increase in the correlation and a gradient closer to 1 can be seen in table 1. A likely explanation for this is that glycine and myo-inositol overlap significantly at 1.5T. As glycine was not present in the default LCModel basis set myo-inositol was being systematically overestimated resulting in a reduced gradient and an increased intercept. Glycine is present in high enough levels in some tumours to warrant being included in the basis set. This illustrates how ^1H HR-MAS data can be used to improve *in-vivo* analysis.

Aspartate and scyllo-inositol were the metabolites with the poorest correlation which is most likely to be due to their typically low concentration in brain tumour tissue. The low concentration combined with the relatively low SNR of *in-vivo* MRS causes a large random variation in their *in-vivo* estimation. Confirmation that these metabolites are poorly quantitated *in-vivo* comes from their CRLB which are the highest of all the metabolites (figure 1). GPC was also poorly correlated ($p=0.23$) despite having a relatively low CRLB of 22% whereas PC is highly correlated with a significance of ($p=0.006$). PC+GPC shows an improved correlation ($p=0.0002$) compared to the individual metabolites which is expected since these signals strongly overlap at 3.2 PPM. This result confirms that the accurate quantitation of PC and

GPC is degraded by interference between the two metabolites, but despite this the results imply that PC can be reliably estimated *in-vivo* in some cases.

Closer inspection of that data revealed that the best agreement for PC between *in-vivo* MRS and *ex-vivo* HR-MAS occurred in the medulloblastoma cases which typically exhibited a large peak *in-vivo* at 3.2ppm which is the dominant spectral feature for this metabolite. The HR-MAS data confirmed this finding and showed that this peak was mainly comprised of PC rather than GPC. This may indicate that LCModel can reliably estimate PC when it has a high signal amplitude compared to the noise level. While it is unlikely that the separation between the PC and GPC singlets at 3.2 PPM is sufficient to distinguish between them, it may be possible that the PC downfield signals can aid more accurate quantitation. These signals are usually indistinguishable from the noise and other overlapping peaks. However the high PC concentration found in medulloblastomas combined with excellent signal to noise ratio, which results from their high cellular density, combine to optimise the spectral characteristics required for detecting the downfield peaks of PC.

As with any method of metabolite quantity scaling, it is possible to observe false correlations when the variation of the quantity of interest is much smaller than the variation in the scaling quantity. To reduce this potential bias the summation of three metabolites was used for scaling. The choice of using multiple metabolites as a scaling quantity was taken to reduce the chance of one metabolite dominating the scaling. Ideally the summation of all metabolites in the analysis would be combined, however poorly fitted metabolites with a large variance could potentially add large random variation in the scaling factor.

To check that the metabolite quantities chosen for scaling were not introducing false correlation, a box-and-whisker diagram is shown in figure 6. Creatine, myo-inositol+glycine and total choline do not show significantly higher variation than the other metabolite quantities indicating that there is a low chance of observing false correlations. In addition, Scyllo and Asp were the metabolites with the lowest

scaled quantity and were also poorly correlated (shown in Table 1). This indicates that the metabolites most susceptible to false correlation were not affected.

4 Conclusions

This study has shown that generally a good correlation exists between metabolite quantities detected by *ex-vivo* ^1H HR-MAS and *in-vivo* MRS for the tumours studied. This indicates that removing tumour tissue from the body does not cause significant alterations in the metabolite quantities observed and that significant metabolite heterogeneity was not present in the tumours investigated. Results also suggest that heavily overlapping metabolites can be accurately quantitated with *in-vivo* MRS in favourable cases. Intuitively, metabolites at lower concentration showed the least agreement between the methods, implying that low SNR is a significant source of error for *in-vivo* MRS.

The enhanced resolution and SNR of ^1H HR-MAS data showed a clearer separation between different metabolite signals as well as revealing numerous signals which were not visible in the *in-vivo* MRS data. This indicates that a more complete and accurate metabolite profile can be obtained from ^1H HR-MAS. In general, this comparison provides some validation for both *in-vivo* MRS and *ex-vivo* HR-MAS studies and highlights that *in-vivo* MRS and *ex-vivo* ^1H HR-MAS can be used as complementary techniques.

5 Acknowledgements

Martin Wilson and Nigel Davies were funded by eTUMOUR. Andrew Peet held a Department of Health Clinical Scientist Award. HR-MAS was carried out in the Henry Wellcome Building for Biomolecular NMR Spectroscopy, University of Birmingham.

References

1. Choi CG and Frahm J. Localized proton MRS of the human hippocampus: metabolite concentrations and relaxation times. *Magn Reson Med* 1999; **41**(1): 204–7.
2. Panigrahy A, Nelson MD Jr, Finlay JL, Sposto R, Krieger MD, Gilles FH and Bluml S. Metabolism of diffuse intrinsic brainstem gliomas in children. *Neuro Oncol* 2008; **10**(1): 32–44.
3. Cordery RJ, MacManus D, Godbolt A, Rossor MN and Waldman AD. Short TE quantitative proton magnetic resonance spectroscopy in variant Creutzfeldt-Jakob disease. *Eur Radiol* 2006; **16**(8): 1692–8.
4. Staffen W, Zauner H, Mair A, Kutzelnigg A, Kapeller P, Stangl H, Raffer E, Niederhofer H and Ladurner G. Magnetic resonance spectroscopy of memory and frontal brain region in early multiple sclerosis. *J Neuropsychiatry Clin Neurosci* 2005; **17**(3): 357–63.
5. Chang L, Lee PL, Yiannoutsos CT, Ernst T, Marra CM, Richards T, Kolson D, Schifitto G, Jarvik JG, Miller EN, Lenkinski R, Gonzalez G and Navia BA. A multicenter in vivo proton-MRS study of HIV-associated dementia and its relationship to age. *Neuroimage* 2004; **23**(4): 1336–47.
6. Frederick BD, Lyoo IK, Satlin A, Ahn KH, Kim MJ, Yurgelun-Todd DA, Cohen BM and Renshaw PF. In vivo proton magnetic resonance spectroscopy of the temporal lobe in Alzheimer’s disease. *Prog Neuropsychopharmacol Biol Psychiatry* 2004; **28**(8): 1313–22.
7. Peet AC, Davies NP, Ridley L, Brundler MA, Kombogiorgas D, Lateef S, Nataraajan K, Sgouros S, MacPherson L and Grundy RG. Magnetic resonance spectroscopy suggests key differences in the metastatic behaviour of medulloblastoma. *Eur J Cancer* 2007; **43**: 1037–1044.

8. Panigrahy A, Krieger MD, Gonzalez-Gomez I, Liu X, McComb JG, Finlay JL, Nelson MD Jr, Gilles FH and Bluml S. Quantitative short echo time ^1H -MR spectroscopy of untreated pediatric brain tumors: preoperative diagnosis and characterization. *AJNR Am J Neuroradiol* 2006; **27**(3): 560–72.
9. Astrakas LG, Zurakowski D, Tzika AA, Zarifi MK, Anthony DC, De Girolami U, Tarbell NJ and Black PM. Noninvasive magnetic resonance spectroscopic imaging biomarkers to predict the clinical grade of pediatric brain tumors. *Clin Cancer Res* 2004; **10**: 8220–8228.
10. Provencher SW. Estimation of metabolite concentrations from localized in vivo proton NMR spectra. *Magn Reson Med* 1993; **30**(6): 672–9.
11. Cheng LL, Becerra L, Ptak T, Tracey I, Lackner A and Gonzalez RG. Quantitative neuropathology by high resolution magic angle spinning proton magnetic resonance spectroscopy. *Proc Natl Acad. Sci* 1996; **96**: 1023–1031.
12. Sitter B, Sonnewald U, Spraul M, Fjosne HE and Gribbestad IS. High-resolution magic angle spinning MRS of breast cancer tissue. *NMR Biomed* 2002; **15**(5): 327–37.
13. Sitter B, Lundgren S, Bathen TF, Halgunset J, Fjosne HE and Gribbestad IS. Comparison of HR MAS MR spectroscopic profiles of breast cancer tissue with clinical parameters. *NMR Biomed* 2006; **19**(1): 30–40.
14. Lyng H, Sitter B, Bathen TF, Jensen LR, Sundfor K, Kristensen GB and Gribbestad IS. Metabolic mapping by use of high-resolution magic angle spinning ^1H MR spectroscopy for assessment of apoptosis in cervical carcinomas. *BMC Cancer* 2007; **7**: 11.
15. Yang Y, Li C, Nie X, Feng X, Chen W, Yue Y, Tang H and Deng F. Metabonomic studies of human hepatocellular carcinoma using high-resolution magic-angle

- spinning ^1H NMR spectroscopy in conjunction with multivariate data analysis. *J Proteome Res* 2007; **6**(7): 2605–14.
16. Martinez-Granados B, Monleon D, Martinez-Bisbal MC, Rodrigo JM, del Olmo J, Lluch P, Ferrandez A, Marti-Bonmati L and Celda B. Metabolite identification in human liver needle biopsies by high-resolution magic angle spinning ^1H NMR spectroscopy. *NMR Biomed* 2006; **19**(1): 90–100.
 17. Martinez-Bisbal MC, Marti-Bonmati L, Piquer J, Revert A, Ferrer P, Llacer JL, Piotto M, Assemat O and Celda B. ^1H and ^{13}C HR-MAS spectroscopy of intact biopsy samples ex vivo and in vivo ^1H MRS study of human high grade gliomas. *NMR Biomed* 2004; **17**: 191–205.
 18. Tzika AA, Astrakas L, Cao H, Mintzopoulos D, Andronesi OC, Mindrinos M, Zhang J, Rahme LG, Blekas KD, Likas AC, Galatsanos NP, Carroll RS and Black PM. Combination of high-resolution magic angle spinning proton magnetic resonance spectroscopy and microscale genomics to type brain tumor biopsies. *Int J Mol Med* 2007; **20**(2): 199–208.
 19. Barton SJ, Howe FA, Tomlins AM, Cudlip SA, Nicholson JK, Bell BA and Griffiths JR. Comparison of in vivo ^1H MRS of human brain tumours with ^1H HR-MAS spectroscopy of intact biopsy samples in vitro. *MAGMA* 1999; **8**(2): 121–8.
 20. E Sjobakk T, Johansen R, Bathen TF, Sonnewald U, Juul R, Torp SH, Lundgren S and Gribbestad IS. Characterization of brain metastases using high-resolution magic angle spinning MRS. *NMR Biomed* 2007; .
 21. Tzika AA, Cheng LL, Goumnerova L, Madsen JR, Zurakowski D, Astraks LG, Zarifi MK, Scott RM, Anthony DC, Gonzalez RG and Black P. Biochemical characterization of pediatric brain tumours by using in vivo and ex vivo magnetic resonance spectroscopy. *J Neurosurg* 1996; **96**: 1023–1031.

22. Tugnoli V, Schenetti L, Mucci A, Nocetti L, Toraci C, Mavilla L, Basso G, Rovati R, Tavani F, Zunarelli E, Righi V and Tosi MR. A comparison between in vivo and ex vivo HR-MAS ^1H MR spectra of a pediatric posterior fossa lesion. *Int J Mol Med* 2005; **16**(2): 301–7.
23. Tsang TM, Griffin JL, Haselden J, Fish C and Holmes E. Metabolic characterization of distinct neuroanatomical regions in rats by magic angle spinning ^1H nuclear magnetic resonance spectroscopy. *Magn Reson Med* 2005; **53**(5): 1018–24.
24. Reynolds G, Wilson M, Peet A and Arvanitis TN. An algorithm for the automated quantitation of metabolites in in vitro nmr signals. *Magn Reson Med* 2006; **56**(6): 1211–1219.
25. Kleihues P and Cavanee WK. *World health organization classification of tumours*. International agency for research on cancer, 2000.
26. *Gnumeric version 1.7.8*, <http://www.gnome.org/projects/gnumeric>.

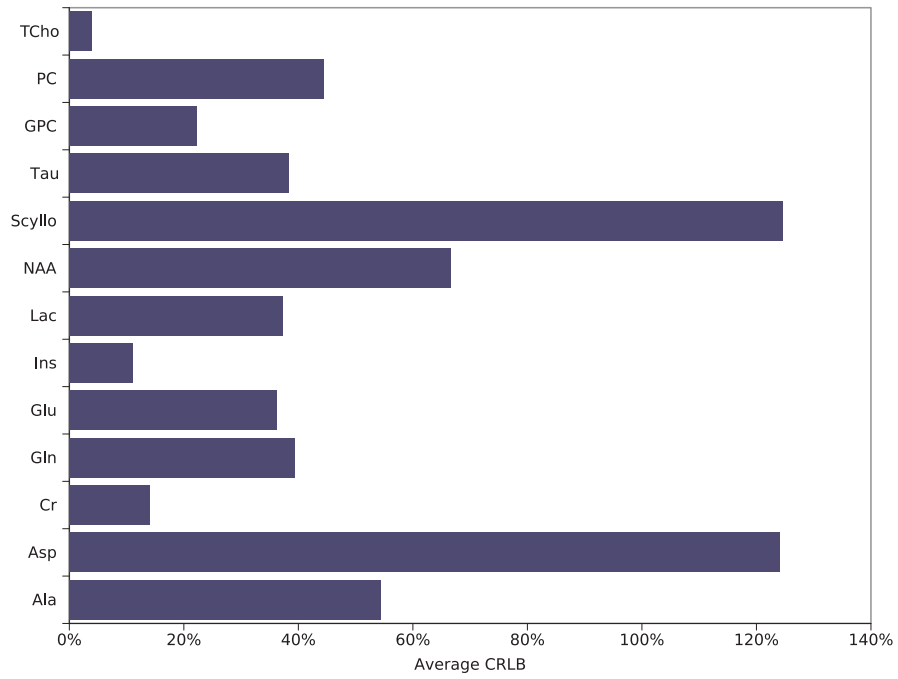


Figure 1: The average CRLB for each metabolite fitted with LCModel.

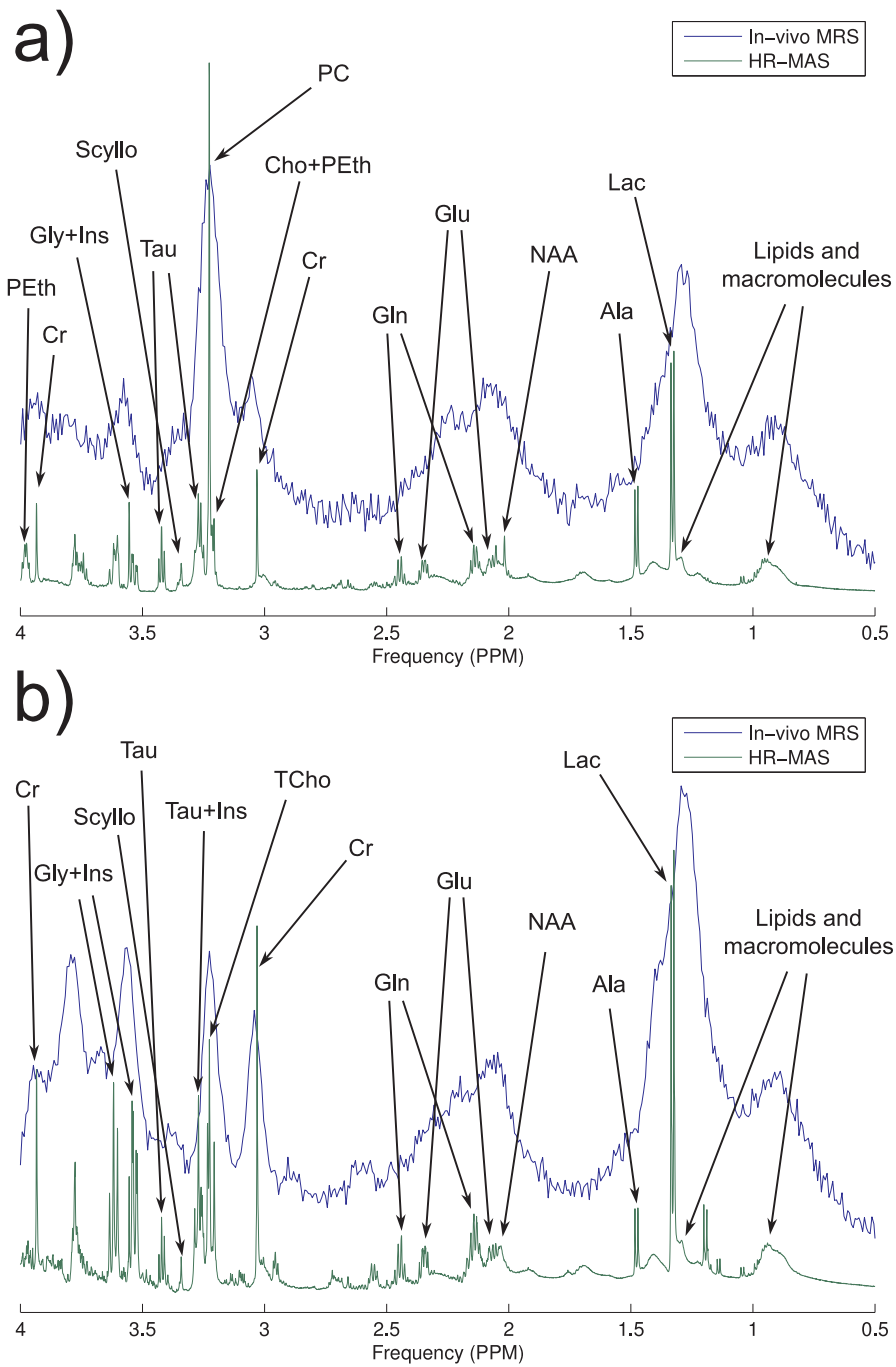


Figure 2: A comparison of ^1H HR-MAS and *in-vivo* MRS spectra for a) medulloblastoma and b) ependymoma tumours.

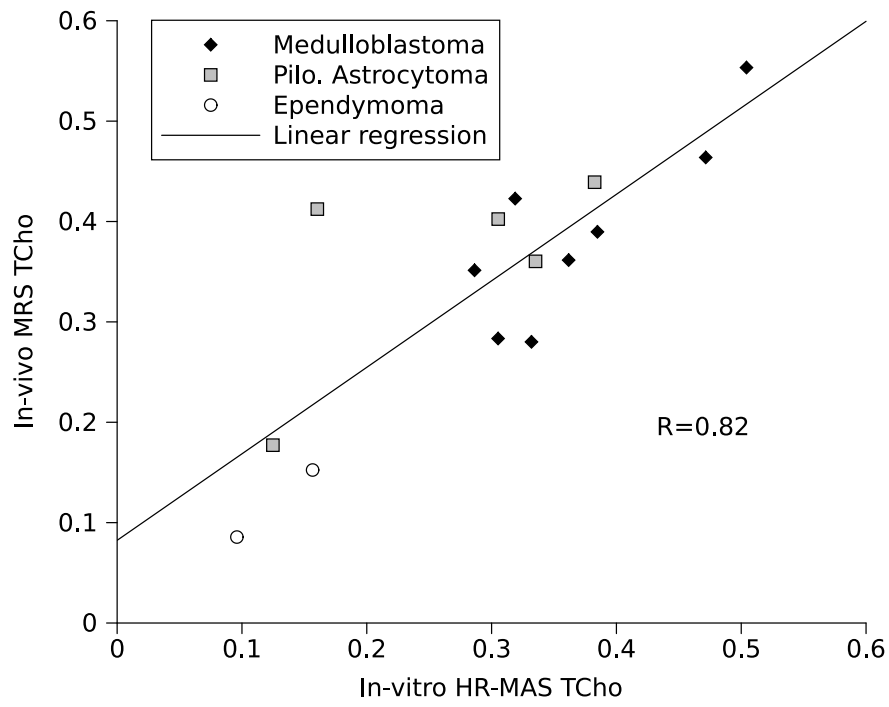


Figure 3: A comparison, of the detected levels of TCho, between *in-vivo* MRS and ^1H HR-MAS.

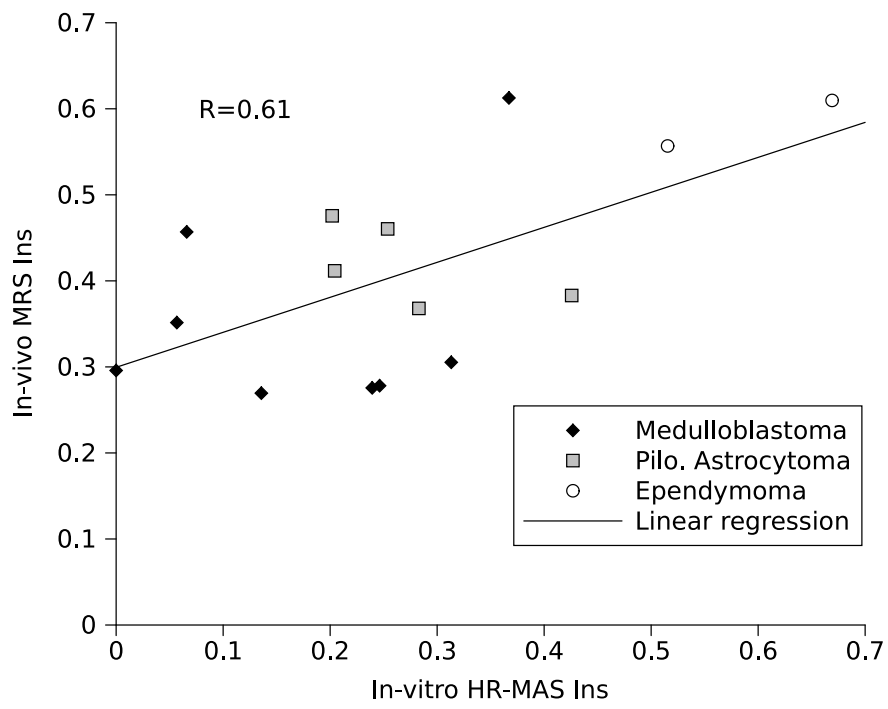


Figure 4: A comparison, of the detected levels of Ins, between *in-vivo* MRS and ^1H HR-MAS.

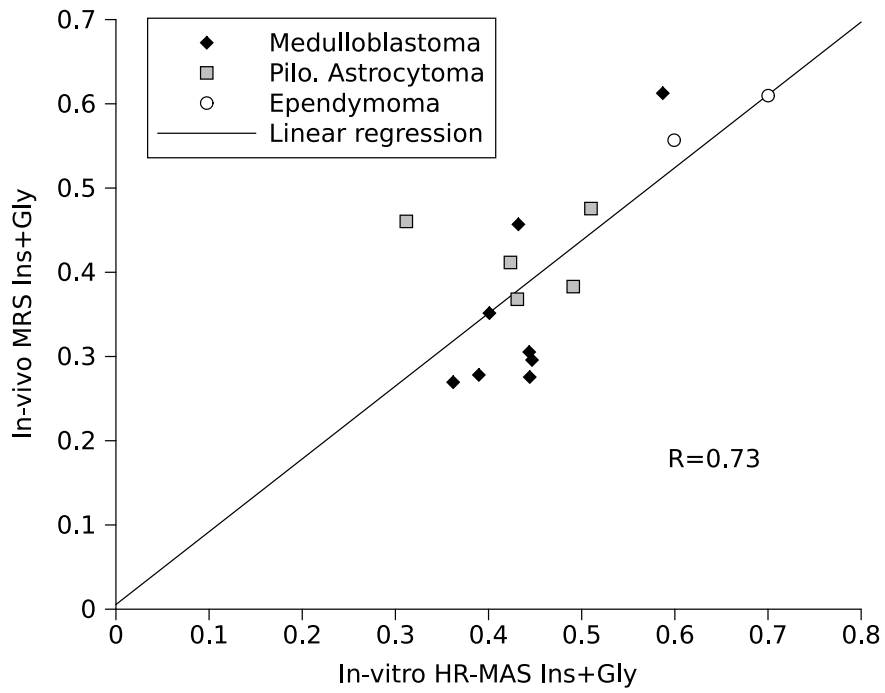


Figure 5: A comparison, of the detected levels of Ins+Gly, between *in-vivo* MRS and ^1H HR-MAS.

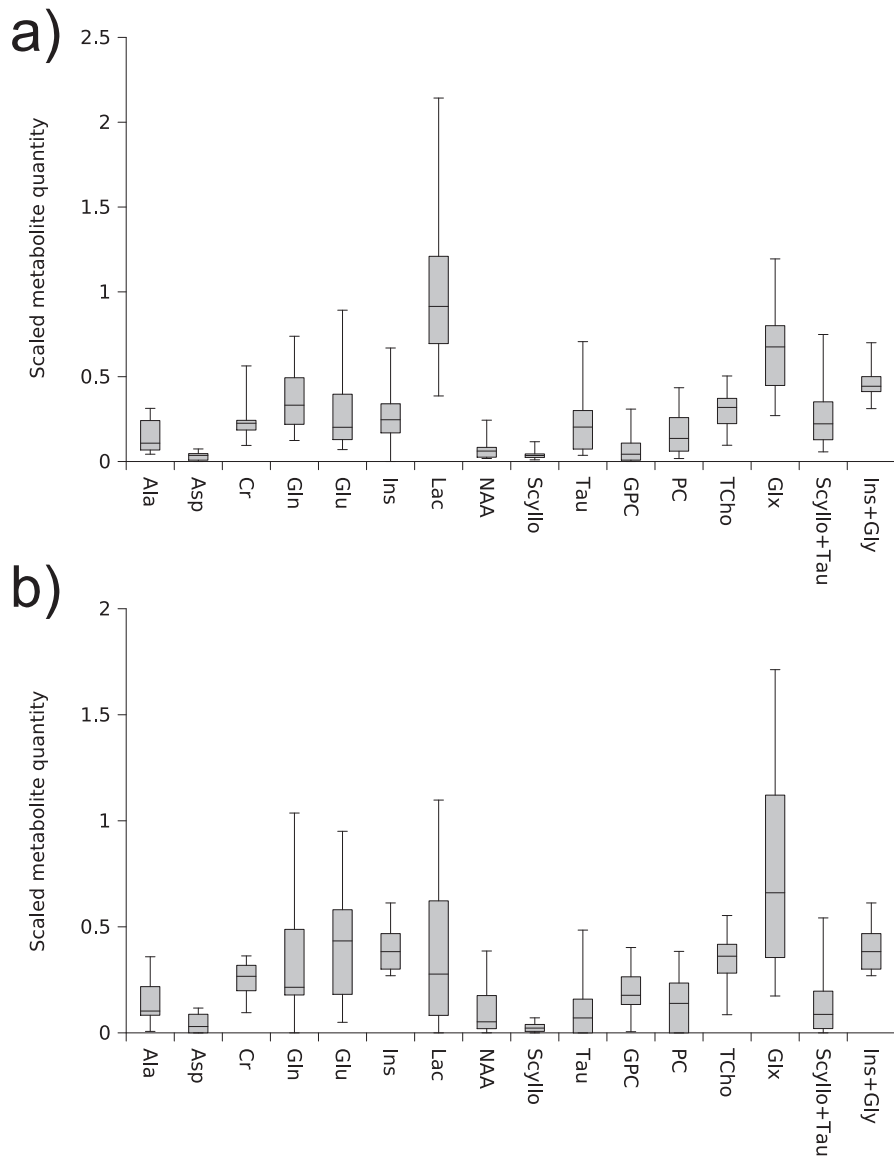


Figure 6: A box-and-whisker diagram of scaled metabolite quantities determined from a) ^1H HR-MAS and b) *in-vivo* MRS data.

Metabolite	p-value	R	m	std error m	c	std error c
Ala	0.0249	0.5750	0.5807	0.2292	0.0620	0.0406
Asp	0.2339	0.3272	0.5750	0.4605	0.0263	0.0185
Cr	0.0344	0.5481	0.4493	0.1901	0.1454	0.0488
Gln	0.0001	0.8409	1.3922	0.2485	-0.1725	0.1053
Glu	0.0075	0.6591	0.8625	0.2730	0.1842	0.0953
Ins	0.0155	0.6110	0.4067	0.1461	0.2995	0.0462
Lac	0.0002	0.8116	0.6309	0.1260	-0.2292	0.1391
NAA	0.0672	0.4844	0.9856	0.4936	0.0423	0.0514
Scyllo	0.2841	-0.2960	-0.2531	0.2266	0.0369	0.0112
Tau	0.0001	0.8432	0.6224	0.1100	-0.0251	0.0302
GPC	0.2265	0.3321	0.4022	0.3168	0.1748	0.0369
PC	0.0063	0.6694	0.6377	0.1963	0.0327	0.0407
TCho	0.0002	0.8242	0.8618	0.1643	0.0824	0.0531
Glx	0.0009	0.7640	1.4866	0.3482	-0.1954	0.2450
Scyllo+Tau	0.0002	0.8137	0.6628	0.1313	-0.0344	0.0403
Ins+Gly	0.0020	0.7296	0.8644	0.2247	0.0055	0.1067

Table 1: Table shows a summary of linear regression results from comparing *ex-vivo* ^1H HR-MAS and *in-vivo* MRS metabolite quantities. R - correlation coefficient, m - gradient of the line of best fit, c - intercept of the line of best fit.